Available online at www.sciencedirect.com
ScienceDirect
Bioorganic & Medicinal Chemistry 15 (2007) 4152–4158
Bioorganic & Medicinal Chemistry

Molecular modeling study for the binding of zonisamide and topiramate to the human mitochondrial carbonic anhydrase isoform VA

Rosa Maria Vitale,[a] Carlo Pedone,[a,b] Pietro Amodeo,[c] Jochen Antel,[d] Michael Wurl,[d] Andrea Scozzafava,[e] Claudiu T. Supuran[e,*] and Giuseppina De Simone[a,*]

[a]*Istituto di Biostrutture e Bioimmagini-CNR, Via Mezzocannone 16, 80134 Naples, Italy*
[b]*Dipartimento delle Scienze Biologiche, University of Naples "Federico II", Via Mezzocannone 16, 80134 Naples, Italy*
[c]*Istituto di Chimica Biomolecolare-CNR, Comprensorio Olivetti, I-80078, Pozzuoli (Naples), Italy*
[d]*Solvay Pharmaceuticals Laboratories, Hans Böckler-Allee 20, D-30173 Hannover, Germany*
[e]*Università degli Studi di Firenze, Polo Scientifico, Laboratorio di Chimica Bioinorganica, Rm. 188, Via della Lastruccia 3, 50019 Sesto Fiorentino (Florence), Italy*

Received 2 November 2006; revised 16 March 2007; accepted 23 March 2007
Available online 30 March 2007

Abstract—Zonisamide and topiramate are two antiepileptic drugs known to induce weight loss in epilepsy patients. These molecules were recently shown to act as carbonic anhydrase (CA) inhibitors, being presumed that the weight loss may be due to the inhibition of the mitochondrial isozymes CA VA and CA VB involved in metabolic processes, among which lipid biosynthesis. To better understand the interaction of these compounds with CAs, here, we report a homology modeling and molecular dynamics simulations study on their adducts with human carbonic anhydrase VA (hCA VA). According to our results, in both cases the inhibitor sulfamate/sulfonamide moiety participates in the canonical interactions with the catalytic zinc ion, whereas the organic scaffold establishes a large number of van der Waals and polar interactions with the active site cleft. A structural comparison of these complexes with the corresponding homologues with human carbonic anhydrase II (hCA II) provides a rationale to the different affinities measured for these drugs toward hCA VA and hCA II. In particular, our data suggest that a narrower active site cleft, together with a different hydrogen bond network arrangement of hCA VA compared to hCA II, may account for the different K_d values of zonisamide and topiramate toward these physiologically relevant hCA isoforms. These results provide useful insights for future design of more isozyme-selective hCA inhibitors with potential use as anti-obesity drugs possessing a novel mechanism of action.

1. Introduction

Selectivity of enzyme inhibitors for closely related enzyme isoforms is particularly important for the drug design of either pharmacological tools or potential drugs. An interesting example is offered by the family of the α-carbonic anhydrases (CAs, EC 4.2.1.1), with at least 16 different isoforms isolated and characterized up to now in humans, which play important physiological and pathological roles.[1,2] Many of these CA isozymes were recently shown to be targets for the drug design of inhibitors with various medicinal chemistry applications. None of the presently available, clinically used CA inhibitors (among which acetazolamide, methazolamide, ethoxzolamide, dichlorophenamide, dorzolamide, or brinzolamide) shows selectivity for a specific isozyme, although their affinity for most of them varies to a large extent.[3]

Among the different applications of this class of pharmacological agents, the possible use of CA inhibitors (CAIs) for the management of obesity is of particular interest, since two of them with antiepileptic effects, namely topiramate (**TPM**)[4] and zonisamide (**ZNS**)[5] (Fig. 1), are known to induce weight loss in epilepsy patients after pharmacological treatment. Moreover, several controlled clinical trials have been performed to evaluate the potential of **TPM** for the treatment of

Keywords: Carbonic anhydrase; Molecular dynamics; Anti-obesity drug.
* Corresponding authors. Tel.: +39 055 4573005; fax: +39 055 4573385 (C.T.S.); tel.: +39 081 2534579; fax: +39 081 2536642 (G.D.S.); e-mail addresses: claudiu.supuran@unifi.it; gdesimon@unina.it

0968-0896/$ - see front matter © 2007 Elsevier Ltd. All rights reserved.
doi:10.1016/j.bmc.2007.03.070

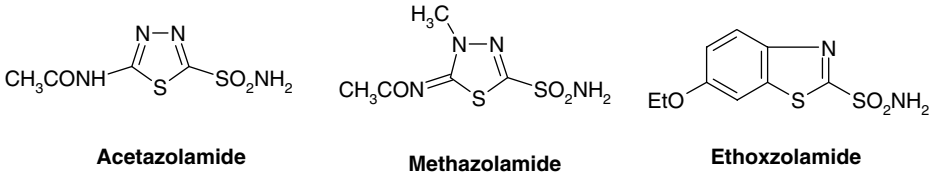

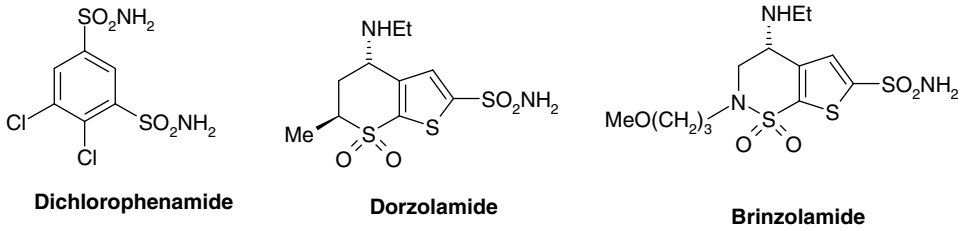

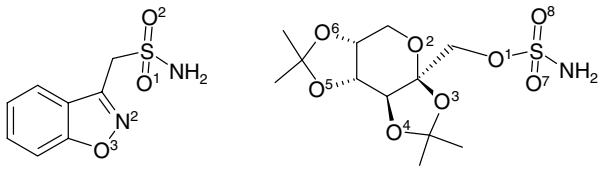

Figure 1. **ZNS** and **TPM** chemical structures.

obesity and metabolic disorders.[6–10] Since using of other CAIs has also been associated with weight loss,[11] it was presumed that some of these actions may be due to the inhibition of the mitochondrial isozymes CA VA and CA VB,[12,13] which are involved in metabolic processes such as the biosynthesis of lipids.[14–16]

Recently, X-ray crystallographic studies showed the binding mode of **ZNS** and **TPM** to hCA II, the most ubiquitous isoform of this enzyme, and one of the most active catalysts known in nature.[4,5] In these studies, it was also reported that while **ZNS** shows a slightly higher affinity for hCA VA than for hCA II in certain experimental conditions (Table 1),[5] **TPM** shows higher affinity for hCA II than for hCA VA.[4] In the present study, these results are explained by means of a modeling investigation on the binding of **ZNS** and **TPM** to hCA VA. These results may bring novel insights into the design of CAIs with selectivity for isoform VA over isoform II.

Table 1. hCA II and hCA VA inhibition data with **ZNS** and **TPM** by means of a spectrophotometric dansylamide binding assay

Compound	K_d[c] (nM)	
	hCA II[a]	hCA VA[b]
ZNS	47.6 ± 2.4	20.6 ± 0.3
TPM	13.8 ± 0.4	25.4 ± 0.6

Inhibitor and enzyme were preincubated for 1 h prior to assay.
[a] Human recombinant enzyme.
[b] Human full length recombinant enzyme.[16]
[c] Mean value from three different determinations.

2. Results and discussion

2.1. Chemistry and CA inhibition

The two antiepileptic drugs **ZNS** and **TPM** contain in their molecules a sulfonamide and a sulfamate group, respectively, and were recently shown to act as effective inhibitors of several CA isozymes.[4,5] Indeed, a host of studies showed that the sulfonamide moiety[3] and its close relatives, the sulfamate[17] and the sulfamide[18] ones, are the most appropriate zinc binding functions in the design of efficient CA inhibitors, targeting isozymes II, VA, VB, VII, IX, XII, and XIV. However, few studies up to now tried to rationalize why the diverse CA isozymes, although structurally quite similar in the inhibitor binding site, show a quite different behavior toward various classes of inhibitors. In the present study, the inhibitory properties of **ZNS** and **TPM** toward hCA II and hCA VA were measured by using a dansylamide competition binding assay.[19] We have measured the two inhibitors in strictly identical experimental conditions, since they greatly influence the inhibitory power (Table 1).

Data reported in Table 1 show that both compounds behave as potent inhibitors against the two investigated CA isoforms, with dissociation constants in the range of 13.8–47.6 nM against hCA II, and 20.6–25.4 nM against hCA VA full length enzyme, respectively. Measured K_d values confirm previous investigations in which a stopped-flow CO_2 hydrase assay was used for monitoring CA II inhibition.[5] According to these data, **ZNS** is a more potent hCA VA inhibitor than hCA II inhibitor (by a factor of 2.3), whereas just the opposite is true for **TPM**, which behaves as a stronger hCA II than hCA VA inhibitor (by a factor of 1.8). The molecular modeling studies we describe later in this paper rationalize these observations which may help the design of more selective CA inhibitors targeting the mitochondrial versus the cytosolic isozyme.

2.2. Modeling studies

A model of G25-Q261 hCA VA domain (hCA I numbering system) was obtained using the available X-ray structure of the corresponding domain from the murine CA V (mCA V) as template[20] and further refined by energy minimization and molecular dynamics simulation as described in Section 4. hCA VA and mCA V share 76% sequence identity (Fig. 2); accordingly, the calculated model should provide a good representation of the molecular structure of hCA VA. As already observed for other α-carbonic anhydrases with solved three-dimensional structure,[21] the hCA VA structural model consists of a central 10-stranded β-sheet surrounded by several helices and additional β-strands (Fig. 3). All geometrical arrangement of the residues coordinating the active site Zn^{2+} and hydrogen bond interactions between zinc ligands and their protein environment are retained. The highly preserved structural fold can be ascribed to the high number of conserved residues between the different hCA isoforms.

As expected, the hCA VA three-dimensional model is very similar to that of hCA II. When superimposing the G25-Q261 hCA VA Cα atoms with those corresponding in isozyme II, a low rms deviation is calculated (1.5 Å). However, an accurate analysis reveals a number of important local structural differences between the two enzymes (Fig. 3). These differences are mainly localized in the N124-G140 region, constituted by a loop/α-helix/loop structure, and are originated by the insertion of S125, and the F131Y and C206S mutations (Figs. 2 and 3). In particular, while the insertion of S125 causes a lengthening of the loop N124-E129, Y131 and S206 are involved in two hydrogen bonds with the Q92 side chain (Y131OH–Q92Nε2) and the amide oxygen of V135 (S206Oγ–V135O), respectively. Thus, both F131Y and C206S mutations affect the orientation of the loop/α-helix/loop region, which moves toward the catalytic Zn^{2+}. As a consequence, the active site cleft is narrower in hCA VA than in hCA II. This tightening seems to be further amplified by the A65L mutation.

On the basis of the high sequence/structural similarity between hCA VA and hCA II, it is not surprising that **ZNS** and **TPM** show only small differences in the affinity toward both enzymes (Table 1). To assess the molecular basis of the small differences observed, the models of the **ZNS**– and **TPM**–hCA VA complexes have been built by homology modeling, refined by energy minimization/molecular dynamics, and then compared with the corresponding **ZNS/TPM** complexes with isoform II. To check the reliability of used computational protocol, molecular dynamics simulations were also carried out starting from the crystallographic structure of **ZNS**– and **TPM**–hCA II complexes, obtaining rmsd values of 1.3 and 1.2 Å, respectively, for the backbone atoms of the region 23–260. These findings, together with the secondary structure comparison of the MD-relaxed structures versus the crystallographic ones, demonstrate the substantial preservation of the hCA II fold and of the inhibitor–protein local interactions within complexes. The energy profile and the backbone rmsd as a function of time, reported in Figure 4, exhibit a quite regular profile, showing that all the simulations are stable on the timescale considered for the subsequent analysis.

The main protein–inhibitor interactions observed in the **ZNS**–hCA II complex after the MD simulation are reported in Figure 5a. A careful analysis of this figure reveals a conserved orientation of the active site

```
hCAVA 18   VPVSVPGGTRQSPINIQWRDSVYDPQLKPLRVSYEAASCLYIWNTGYLFQVEFDDATEA
mCAV  22   ----CATGTRQSPINIQWKDSVYDPQLAPLRVSYDAASCRYLWNTGYFFQVEFDDSCED
hCAII 18   KDFPIAKGERQSPVDIDTHTAKYDPSLKPLSVSYDQATSLRILNNGHAFNVEFDDSQDK

hCAVA 77   SGISGGPLENHYRLKQFHFHWGAVNEGGSEHTVDGHAYPAELHLVHWNSVKYQNYKEAV
mCAV  77   SGISGGPLGNHYRLKQFHFHWGATDEWGSEHAVDGHTYPAELHLVHWNSTKYENYKKAS
hCAII 77   AVLKGGPLDGTYRLIQFHFHWGSLDGQGSEHTVDKKKYAAELHLVHWN-TKYGDFGKAV

hCAVA 136  VGENGLAVIGVFLKLGAHHQTLQRLVDILPEIKHKDARAAMRPFDPSTLLPTCWDYWTY
mCAV  136  VGENGLAVIGVFLKLGAHHQALQKLVDVLPEVRHKDTQVAMGPFDPSCLMPACRDYWTY
hCAII 136  QQPDGLAVLGIFLKVGSAKPGLQKVVDVLDSIKTKGKSADFTNFDPRGLLPESLDYWTY

hCAVA 195  AGSLTTPPLTESVTWIIQKEPVEVAPSQLSAFRTLLFSALGEEEKMMVNNYRPLQPLMN
mCAV  195  PGSLTTPPLAESVTWIVQKTPVEVSPSQLSMFRTLLFSGRGEEEDVMVNNYRPLQPLRD
hCAII 195  PGSLTTPPLLECVTWIVLKEPISVSSEQVLKFRKLNFNGEGEPEELMVDNWRPAQPLKN

hCAVA 254  RKVWASFQATNEGTRS
mCAV  254  RKLRSSFRLDRTKMRS
hCAII 254  RQIKASFK--------
```

Figure 2. Sequence alignment used for modeling hCA VA, showing the sequence of hCA VA in comparison to those of mCA V and hCA II. Residues conserved between hCA VA and mCA V and between hCA II and hCA VA are highlighted in red and magenta, respectively.

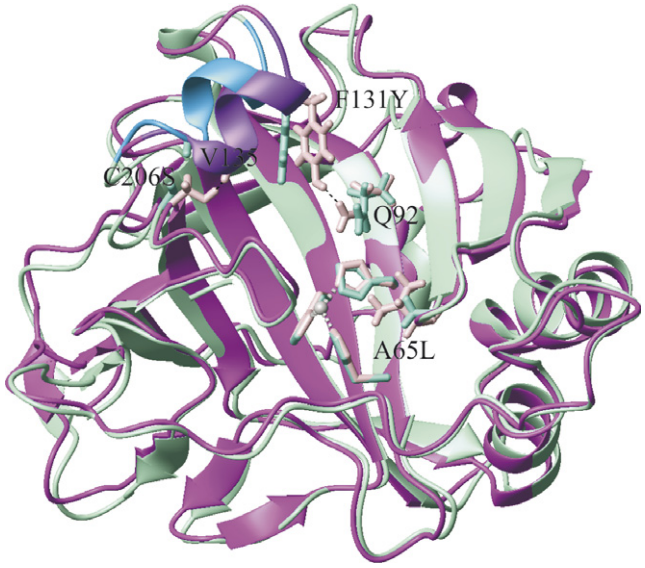

Figure 3. Superposition of the hCA VA homology model (magenta) and the hCA II structure (cyan). The region N124-G140 is highlighted in purple (hCA VA) and light blue (hCA II). The active site Zn^{2+} ion coordination is shown in ball-and-stick representation.

residues, with all conserved H-bonds arranged to ensure proper catalytic efficiency.[20,22] The tetrahedral geometry of the Zn^{2+} binding site and the key hydrogen bonds between the sulfonamide moiety of the inhibitor and the enzyme active site are all retained with respect to the X-ray structure.[5] Finally, as observed in the crystal structure, the benzisoxazole ring of **ZNS** is oriented toward the hydrophobic part of the active site cleft (Fig. 5a), establishing a large number of strong van der Waals interactions with residues Q92, V121, L141, V143, L198, T200, and P201.

All these contacts occur also in **ZNS**–hCA VA complex model (Fig. 5b). On the contrary, a unique polar interaction distinguishes the **ZNS**–hCA VA complex from the hCA II counterpart. In fact, the intramolecular H-bond between the Y131OH group and Q92Nε2, previously described as a unique characteristic of hCA VA enzyme, has in the **ZNS**–hCA VA complex a crucial role in the proper orientation of Q92 side chain and in the consequent formation of a H-bond interaction between the enzyme and the inhibitor (Fig. 5b). In particular, the Q92Nε2 atom forms a H-bond with **ZNS**N2 atom characterized by a high occurrence during the simulation period, and with **ZNS**O3 atom, even if with a minor occurrence. Being a phenylalanine residue present at position 131 in hCA II, this interaction is claimed as the unique structural feature accounting for the observed differences in binding affinity between the two isozymes.

The main protein–inhibitor interactions observed in the **TPM**–hCA II complex after MD simulation are depicted in Figure 6a. According to this figure, **TPM** presents a spatial arrangement similar to that observed in the X-ray structure.[4] In particular, the tetrahedral geometry of the Zn^{2+} binding site and the key hydrogen bonds between the sulfamate moiety of the inhibitor and enzyme active site are all retained. The extended network

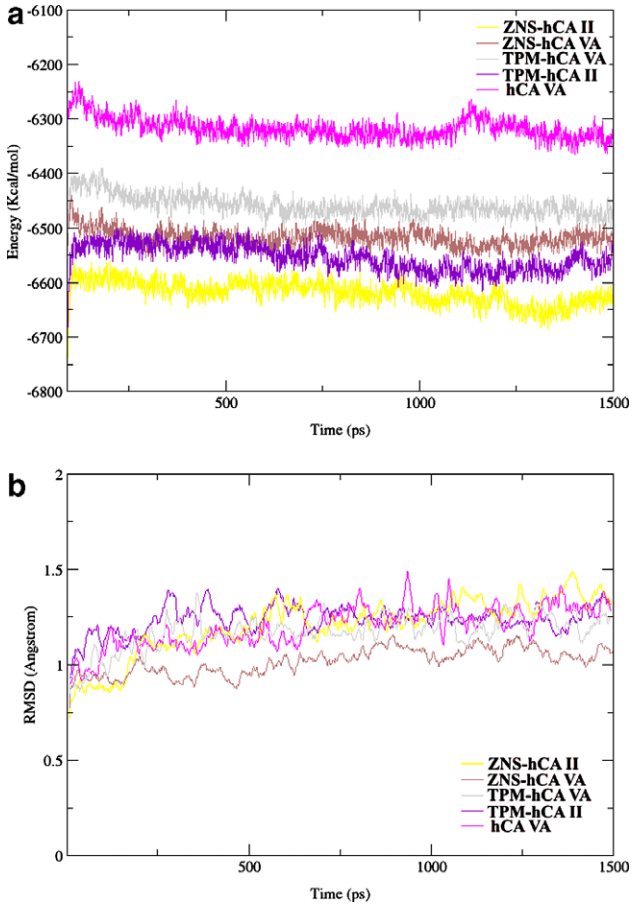

Figure 4. Plot of the potential energy (a) and backbone rmsd (b) versus time during 1.5 ns of MD production run of hCA II bound to **ZNS** and **TPM**, and hCA VA bound to **ZNS**, **TPM** and without inhibitor. Only for hCA II protein the first 19 residues of the flexible N-terminal tail were not included in rmsd calculation.

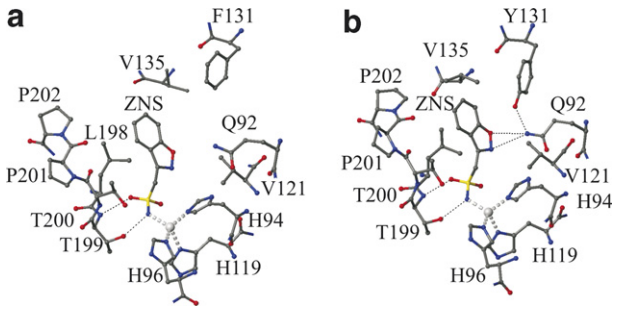

Figure 5. Active site region in the **ZNS**–hCA II (a) and **ZNS**–hCA VA (b) complexes, showing residues participating in recognition of the inhibitor molecules. Hydrogen bonds and the active site Zn^{2+} ion coordination are also shown (dotted lines).

of hydrogen bonds, which in the crystal structure strongly stabilize the organic scaffold of the inhibitor within the enzyme active site, are all retained after MD simulation (Fig. 6a). Such important hydrogen bonds are: N62Nδ2–TPMO6, Q92Nε2–TPMO4, T200Oγ–TPMO2. The analysis of the **TPM**–hCA VA complex after MD simulation reveals that while the sulfamate group of the inhibitor binds to the enzyme active site in

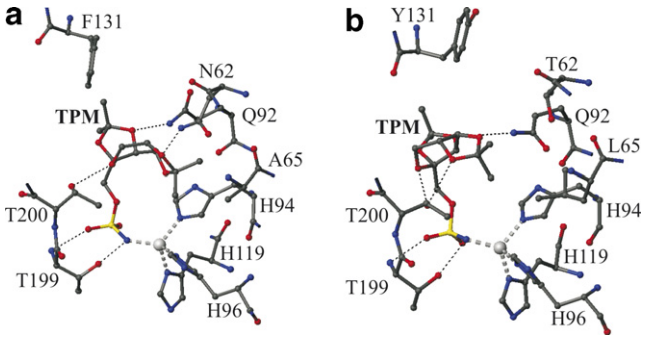

Figure 6. Active site region in the **TPM**–hCA II (a) and **TPM**-hCA VA (b) complexes, showing residues participating in recognition of the inhibitor molecules. Hydrogen bonds and the active site Zn^{2+} ion coordination are also shown (dotted lines).

a manner similar to that observed in the complex with isoform II, a different network of polar interactions of the organic scaffold distinguishes the **TPM**–hCA VA complex from the **TPM**–hCA II one. Only the Q92Nε2–TPMO4 H-bond is conserved in the case of isoform VA. In fact, T200Oγ is now involved in a bifurcated hydrogen bond with TPMO2 and TPMO6 atoms, while the hydrogen bond interaction N62Nδ2–TPMO6 is not retained in this case, as a consequence of the mutation N62T (Figs. 2 and 6b). The loss of this important polar interaction seems to be responsible for the lower binding affinity observed for **TPM** toward hCA VA with respect to that measured for hCA II. During the MD simulations of the complex **TPM**–hCA VA, worthy of noting is also the disappearance of the intramolecular H-bond Y131OH–Q92Nε2, already observed in the hCA VA–**ZNS** complex; this result being dependent on the re-positioning of the Y131 side chain. In fact, the presence of the bulkier **TPM** molecule and the consequent constriction in the enzyme active site causes a partial opening of the N124-G140 region, resulting in the movement of Y131 away from the enzyme active site (Fig. 6b).

3. Conclusion

In conclusion, a homology modeling and molecular dynamics simulations study of the adducts of hCA VA with the two potent inhibitors **TPM** and **ZNS** is here reported. Our results show that in both inhibitors the sulfamate/sulfonamide moiety is involved in classical interactions with the Zn^{2+} ion, whereas the organic scaffold establishes a large number of van der Waals and polar interactions with the active site cleft. A structural comparison with the corresponding complexes with hCA II provides a reasonable explanation for the different measured affinities of **TPM** and **ZNS** toward CA isozymes. Particularly, these results suggest that a different H-bond network arrangement in conjunction with a narrower active site cleft may account for the different K_d values measured for these inhibitors toward hCA VA and hCA II. These data may be instrumental in the design of CA inhibitors selective for isozyme VA, to be further used as anti-obesity drugs.[13]

4. Experimental

4.1. Chemistry and CA inhibition

4.1.1. Materials. Recombinant hCA II and recombinant full length hCA VA were obtained as reported earlier.[23] Buffers, solvents, and salts were from Sigma–Aldrich (Milan, Italy) of highest purity available. Topiramate was from Johnson & Johnson, whereas zonisamide from DaiNippon.

4.1.2. Spectrofluorometric CA inhibition studies. Dansylamide competition binding assays of the two CA isozymes and the test compounds **TPM** and **ZNS** have been performed by the method of Chen and Kernohan,[19] originally designed for measuring CA II inhibition with aromatic/heteroaromatic sulfonamides. The spectrofluorometric studies were performed on a Perkin-Elmer lambda 50-BB spectrofluorometer equipped with a magnetic stirrer and thermostated water bath. The dansylamide stock solution (1 mM) was prepared in 10 mM HCl and diluted in the standard Hepes (10 mM) buffer containing 10% acetonitrile. The emission spectra of dansylamide in the absence and in the presence of hCA II and hCA VA were acquired by fixing the excitation wavelength at 330 nm, and both excitation and emission slits were maintained at 5 mm with a cutoff filter at 390 nm. The dissociation constants of the hCA II–dansylamide and hCA VA–dansylamide complexes were determined by titrating a fixed concentration of the enzyme (0.1 μM) with increasing concentrations of dansylamide in different pH buffers, containing 10% acetonitrile. The initial reaction volume was 1.0 mL. To maximize the signal-to-noise ratio as well as to minimize the fluorescence drift, the excitation and emission wavelengths were maintained at 330 and 448 nm, respectively. The excitation and emission slits were of 5 mm each. The dissociation constant of the enzyme–dansylamide complex was determined by analyzing the binding isotherm as described by Lesburg et al.[24] The fluorescence change of the enzyme–dansylamide complexes was then monitored by adding increasing concentrations of sulfonamide/sulfamate inhibitors (starting from 0.1 nM to 10 μM), and the inhibition constants were determined as reported by Chen and Kernohan.[19]

4.2. Modeling

The hCA VA sequence was retrieved from publicly available sequence database Swiss-Prot/TrEMBL (primary accession number P35218).[25] On the base of sequence search against the PDB by using PSI-BLAST,[26] the crystallographic structure of mCA V at 2.45 Å of resolution (PDB code 1DMY)[20] was identified as the best structural template (76% sequence identity) to model the corresponding catalytic domain (G25-Q261) of hCA VA. The alignment of the template and target sequences was carried out with CLUSTALW version 1.83.[27]

Fifty homology models were built with MODELLER[28] and their quality was assessed by using PROCHECK.[29]

The best model in terms of both MODELLER objective target function and PROCHECK g-factor was used to build both the native form of hCA VA (**WAT**–hCA VA), where the Zn^{2+} ion was coordinated to a water molecule, and the starting **ZNS**– and **TPM**–hCA VA complexes. **WAT**–hCA VA and the two inhibitor complexes were obtained by superimposing the three Zn^{2+} coordination histidine residues of hCA VA model onto the corresponding atoms of native hCA II (pdb entry 1CA2),[22] **ZNS**– and **TPM**–hCA II complex structures, respectively.[4,5] Each complex was completed by addition of all hydrogen atoms.

4.3. Molecular dynamics

Molecular dynamics simulations were performed with AMBER8 suite of programs,[30] using the parm99-MOD2 force field.[31] Atomic charges of **ZNS** and **TPM** molecules were obtained with the RESP methodology.[32] The X-ray structure of each inhibitor, deriving from the corresponding complex with hCA II, was fully optimized using GAMESS program[33] at the Hartree–Fock level with the STO-3G basis set. Single-point calculations on each optimized molecule were performed at the RHF/6-31G* level. The resulting electrostatic potentials were thus used for the two-stage single-conformation RESP charge fitting. Partial charges for the three histidines, the coordination water molecule, and the Zn^{2+} ion were those published by Suarez and Merz.[34] To preserve integral charge of the whole system, the partial charges of Cα and Hα atoms of the Zn^{2+} ligands and of N and H atoms of inhibitor sulfonamide groups were modified accordingly. A bonded approach between Zn^{2+} ion and its ligands ensured the experimentally observed tetrahedral Zn^{2+} coordination of the complexes during MD simulations. Equilibrium bond distances and angles were taken from hCA II crystal structures.[4,5] Force constant values of 20 and 30 kcal/(mol Å) were used for N(His)–Zn^{2+}–N(His) and N(His)–Zn–N(sulfonamide) angle bending parameters, respectively. All the torsional parameters associated with the Zn^{2+} ligand interactions were set to zero as in Hoops et al.[35]

The GB^{OBC}/SA methodology[36] was used to represent solvation effects. Hydrogen-involving bond distances were restrained with the SHAKE approach.[37] The MD integration time-step was 1.5 fs, with a cutoff of 16 Å for non-bonded interactions. Each simulation started with 2000 steps of conjugate gradients energy minimization, followed by 60 ps of MD equilibration, during which the temperature was gradually raised from 10 to 300K. The protein atom coordinates were harmonically restrained at their original positions, with force constant values of 5 kcal/mol^{-1} $Å^{-2}$ during minimization and 1 kcal/mol^{-1} $Å^{-2}$ during equilibration. Constraints were subsequently removed, and the production run was carried out at 300K for 1.5 ns. Overall translational and rotational motion was removed every 500 steps. The snapshots were saved every 1000 steps and analyzed with MOLMOL program.[38] Simulations were performed on a 8-CPU cluster with AMD Opteron processors.

References and notes

1. Supuran, C. T. In *Carbonic Anhydrase—its Inhibitors and Activators*; Supuran, C. T., Scozzafava, A., Conway, J., Eds.; CRC: Boca raton, 2004; pp 1–24.
2. Pastorekova, S.; Parkkila, S.; Pastorek, J.; Supuran, C. T. *J. Enzyme Inhib. Med. Chem.* **2004**, *19*, 199.
3. Supuran, C. T.; Casini, A.; Scozzafava, A. In *Carbonic Anhydrase—its Inhibitors and Activators*; Supuran, C. T., Scozzafava, A., Conway, J., Eds.; CRC: Boca raton, 2004; pp 67–148.
4. Casini, A.; Antel, J.; Abbate, F.; Scozzafava, A.; David, S.; Waldeck, H.; Schafer, S.; Supuran, C. T. *Bioorg. Med. Chem. Lett.* **2003**, *13*, 841.
5. De Simone, G.; Di Fiore, A.; Menchise, V.; Pedone, C.; Antel, J.; Casini, A.; Scozzafava, A.; Wurl, M.; Supuran, C. T. *Bioorg. Med. Chem. Lett.* **2005**, *15*, 2315.
6. Tonstad, S.; Tykarski, A.; Weissgarten, J.; Ivleva, A.; Levy, B.; Kumar, A.; Fitchet, M. *Am. J. Cardiol.* **2005**, *96*, 243.
7. Astrup, A.; Toubro, S. *Obes. Res.* **2004**, *12*, 167S.
8. McElroy, S. L.; Shapira, N. A.; Arnold, L. M.; Keck, P. E.; Rosenthal, N. R.; Wu, S. C.; Capece, J. A.; Fazzio, L.; Hudson, J. I. *J. Clin. Psychiatry* **2004**, *65*, 1463, Erratum in: J. Clin. Psychiatry. **2005**, *66*, 138.
9. Astrup, A.; Caterson, I.; Zelissen, P.; Guy-Grand, B.; Carruba, M.; Levy, B.; Sun, X.; Fitchet, M. *Obes. Res.* **2004**, *12*, 1658.
10. Wilding, J.; Van Gaal, L.; Rissanen, A.; Vercruysse, F.; Fitchet, M. *OBES-002. Int. J. Obes. Relat. Metab. Disord.* **2004**, *28*, 1399.
11. Supuran, C. T.; Scozzafava, A. *Expert Opin. Ther. Pat.* **2000**, *10*, 575.
12. Nishimori, I.; Vullo, D.; Innocenti, A.; Scozzafava, A.; Mastrolorenzo, A.; Supuran, C. T. *J. Med. Chem.* **2005**, *48*, 7860.
13. Hebebrand, J.; Antel, J.; Preuschoff, U.; David, S.; Sann, H.; Weske, M. *Int. Patent Appl.* WO 2002007821, **2002**.
14. Supuran, C. T. *Expert Opin. Ther. Pat.* **2003**, *13*, 1545.
15. Hazen, S. A.; Waheed, A.; Sly, W. S.; LaNoue, K. F.; Lynch, C. J. *FASEB J.* **1996**, *10*, 481.
16. Lynch, C. J.; Fox, H.; Hazen, S. A.; Stanley, B. A.; Dodgson, S.; Lanoue, K. F. *Biochem. J.* **1995**, *310*, 197.
17. Winum, J.-Y.; Scozzafava, A.; Montero, J.-L.; Supuran, C. T. *Med. Res. Rev.* **2005**, *25*, 186.
18. Winum, J.-Y.; Scozzafava, A.; Montero, J.-L.; Supuran, C. T. *Expert Opin. Ther. Pat.* **2006**, *16*, 27.
19. Chen, R. F.; Kernohan, J. C. *J. Biol. Chem.* **1967**, *242*, 5813.
20. Boriack-Sjodin, P. A.; Heck, R. W.; Laipis, P. J.; Silverman, D. N.; Christianson, D. W. *Proc. Natl. Acad. Sci. U.S.A.* **1995**, *92*, 10949.
21. Stams, T.; Christianson, D. W. *EXS* **2000**, *90*, 159.
22. Eriksson, A. E.; Jones, T. A.; Liljas, A. *Protein Struct. Funct.* **1988**, *4*, 274.
23. Innocenti, A.; Antel, J.; Wurl, M.; Scozzafava, A.; Supuran, C. T. *Bioorg. Med. Chem. Lett.* **2004**, *14*, 5703.
24. Lesburg, C. A.; Huang, C.-C.; Christianson, D. W.; Fierke, C. A. *Biochemistry* **1997**, *36*, 15780.
25. Boeckmann, B.; Bairoch, A.; Apweiler, R.; Blatter, M. C.; Estreicher, A.; Gasteiger, E.; Martin, M. J.; Michoud, K.; O Donovan, C.; Phan, I.; Pilbout, S.; Schneider, M. *Nucleic Acids Res.* **2003**, *31*, 365.
26. Altschul, S. F.; Madden, T. L.; Schaffer, A. A.; Zhang, J.; Zhang, Z.; Miller, W.; Lipman, D. J. *Nucleic Acids Res.* **1997**, *25*, 3389.
27. Thompson, J. D.; Higgins, D. G.; Gibson, T. J. *Nucleic Acids Res.* **1994**, *22*, 4673.
28. Sali, A.; Blundell, T. J. *J. Mol. Biol.* **1993**, *234*, 779.

29. Laskowski, R. A.; MacArthur, M. W.; Moss, D. S.; Thornton, J. M. *J. Appl. Crystallogr.* **1993**, *26*, 283.
30. Pearlman, D. A.; Case, D. A.; Caldwell, J. W.; Ross, W. S.; Cheatham, T. E., III; DeBolt, S.; Ferguson, D.; Seibel, G.; Kollman, P. *Com. Phys. Commun.* **1995**, *91*, 1.
31. Simmerling, C.; Strockbine, B.; Roitberg, A. E. *J. Am. Chem. Soc.* **2002**, *124*, 11258.
32. Bayly, C. I.; Cieplak, P.; Cornell, W. D.; Kollman, P. A. *J. Phys. Chem.* **1993**, *97*, 10269.
33. Schmidt, M. W.; Baldridge, K. K.; Boatz, J. A.; Elbert, S. T.; Gordon, M. S.; Jensen, J. J.; Koseki, S.; Matsunaga, N.; Nguyen, K. A.; Su, S.; Windus, T. L.; Dupuis, M.; Montgomery, J. A. *J. Comput. Chem.* **1993**, *14*, 1347.
34. Suarez, D.; Merz, K. M. *J. Am. Chem. Soc.* **2001**, *123*, 3759.
35. Hoops, S. C.; Anderson, K. W.; Merz, K. M. *J. Am. Chem. Soc.* **1991**, *113*, 8262.
36. Onufriev, A.; Bashford, D.; Case, D. A. *Proteins* **2004**, *55*, 383.
37. Ryckaert, J.-P.; Ciccotti, G.; Berendsen, H. J. C. *J. Comput. Phys.* **1977**, *23*, 327.
38. Koradi, R.; Billeter, M.; Wuthrich, K. J. *Mol. Graph.* **1996**, *14*, 51.